

Monte-Carlo Simulations of Electron Channeling: a Bent (110) Channel in Silicon

Andriy Kostyuk

65933 Frankfurt am Main, Germany

the date of receipt and acceptance should be inserted later

Abstract. Results obtained with a new Monte-Carlo code ChaS for channeling of 855 MeV electrons along the crystallographic plane (110) in a bent silicon crystal are presented. The dependence of the dechanneling length and the asymptotic acceptance of the channel on the crystal bending is studied.

PACS. XX.XX.XX No PACS code given

1 Introduction

In this article, channeling of ultrarelativistic electrons in a bent planar channel is studied using the Monte-Carlo method.

Channeling has been intensively investigated since the sixties years of the last century. This phenomenon is observed if particles enter a single crystal at a small angle with respect to a major crystallographic direction [1]. Due to the electrostatic potential of the crystal constituents, charged projectiles move preferably along the corresponding crystallographic planes or axes following their shape.

This suggested the idea [2] to use crystals with bent crystallographic planes to steer high-energy charged particle beams. Since its successful experimental verification [3], this idea has been inducing growing interest to practical applications of channeling and related phenomena (e.g. volume capture [4] and volume reflection [5]).

In particular, bent crystals are replacing huge dipole magnets in the Institute for High Energy Physics in Protvino (Russia) where they are used for beam extraction and deflection [6]. A series of experiments on the bent crystal deflection and collimation of proton and heavy ion beams were performed in other laboratories [7, 8, 9, 10, 11, 12] (see also a recent review [13] and references therein). It was proposed to extract particles from the beam halo at Large Hadron Collider using bent crystals [14]. The possibility of deflecting positron [15] and electron [10, 16, 17] beams has been studied as well.

Another interesting application of the channeling phenomenon is the crystalline undulator, a novel source of hard electromagnetic radiation. A single crystal with periodically bent crystallographic planes can force channeling particles to move along nearly sinusoidal trajectories and radiate in the hard x-ray and gamma-ray frequency range [18, 19]. The extremely strong electrostatic fields inside the crystal are able to steer the particles much more effectively than even the most advanced superconductive

magnets. Due to this fact, the period of a crystalline undulator can be made very short (up to several microns¹) and, therefore, the energy of emitted photons can be in the range of several MeV or even higher.

Using positron beams with the crystalline undulator is preferable [21], because positrons have much larger dechanneling length than electrons. On the other hand, electron beams are more easily available and are usually of higher quality and intensity. For this reason, the electron based crystalline undulator [22, 23] may have some practical advantages and, therefore, it deserves a thorough analysis.

Understanding the behavior of charged particles in a bent crystal channel is a necessary step towards developing a comprehensive theory of the crystalline undulator. In the present paper, channeling of electrons in a bent silicon crystal is studied using a new Monte-Carlo code ChaS (**C**hanneling **S**imulator). The code enables one to simulate channeling of charged particles and analyze their trajectories. In contrast to most of other channeling codes [24, 25, 26, 27, 28, 29, 30], the underlying algorithm is not based on the continuous potential approximation. Instead, binary collisions of the projectile with crystal constituents, nuclei and electrons, are simulated. This feature may be especially beneficial in the case of negatively charged projectiles, which channel in the vicinity of the atomic nuclei, where using the continuous potential approximation is not well justified.

The binary collision algorithm is not new in the channeling physics. In fact, it has been actively used in the field since 1960s [31, 32, 33, 34, 35]. But the previously existing codes consider binary collisions of the projectile with the crystal atoms as whole ignoring incoherent collisions with atomic electrons. In contrast, the algorithm of ChaS takes into account collisions of the projectile with target elec-

¹ Recently, it was found [20] that even smaller crystalline undulator periods (hundreds of nanometers) are feasible and advantageous.

trons as well as with nuclei. This is important for positrons as well as for electrons. The absolute contribution of the incoherent scattering by target electrons is expected to be larger in the case of negatively charged projectiles, that have to cross the crystal plane in the process of channeling where the electron density is higher than average. But its relative contribution is larger for positively charged projectiles, that channels between the planes and, therefore, are being incoherently scattered mostly by target electrons.

The scope of the present paper is restricted to the analysis of channels with constant curvature. The results on channeling of 855 MeV electrons in a straight and bent single crystals of silicon along the plane (110) are presented. This plane is chosen for the analysis because it can be deformed by growing of $\text{Si}_{1-x}\text{Ge}_x$ crystals [36] with a varying Ge content x [37,38]. The electron energy corresponds to the conditions of the channeling experiments at Mainz Microtron (Germany) [39,40]. The results will help one to estimate the reasonable parameters of periodically bent crystal channels and, therefore, will facilitate future simulations and experimental study of the electron-based crystalline undulator. Additionally, the results can be useful to developers of crystalline devices for extraction, bending and collimation of electron beams.

2 The Physical Model and the Simulation Algorithm

A detailed description of the physical model and the algorithm that are implemented in the Monte Carlo code ChaS can be found in [41]. In the present section, the basic ideas of the model are briefly reviewed. The part of the algorithm that is relevant to the simulation of a bent crystal is considered in greater details.

The model is optimized for studying the interaction of ultrarelativistic projectiles with single crystals. Due to the high speed of the projectile, its interaction time with a crystal atom is very short. The motion of the atomic electrons as well as the thermal motion of the atomic nuclei during the interaction time can be neglected. Therefore, the crystal is represented as a set of static charges. The atomic nuclei are ‘frozen’ at random positions in the vicinity of nodes of the crystal lattice. The probability distribution of the position of the nucleus relative to the node is approximated by a three dimensional Gaussian distribution. The variance of the distribution is equal to the squared amplitude of thermal vibrations of the crystal atoms $a(T)$. The same value as in [41], $a(T) = 0.075 \text{ \AA}$, is used in the present calculations. It corresponds to the room temperature [42].

The probability distribution of electrons in the crystal is approximated by, a spherically symmetric distribution of Z electrons around each atom (Z is the atomic number). The radial dependence of the distribution is chosen in such a way that it reproduces on average the electrostatic potential of the atom in Molière’s approximation [43].

The code performs 3D simulation of the projectile motion in the crystal. The coordinate frame is defined in such a way that the axis z coincides with the beam direction. The tangent plane to the bent crystallographic plane (110) at the crystal entrance is parallel to the coordinate plane (xz) and, consequently, it is orthogonal to the axis y .

The orientation of the plane is carefully chosen to avoid collinearity of major crystal axes with the coordinate axis z (otherwise axial channeling would be simulated instead of the planar one). The axes are considered to be ‘major’ if the maximum distance between the corresponding atomic strings in the plane (110) exceeds the amplitude of thermal vibrations $a(T)$ by the factor of 3 at least. The orientation of the plane is done in such a way that the angle between such axes and the coordinate axis z is not smaller than $\sim 10 \text{ mrad}$.

The interaction of the projectile with a crystal constituent is considered as a classical scattering in a Coulomb field of a static point-like charge. Electrons and nuclei are taken into account if they belong to a lattice node located within a cylinder of the radius $40a_{\text{TF}}$ around the projectile trajectory (a_{TF} is the Thomas-Fermi radius of the atom). Initially, the straight line along the direction of the projectile momentum at the point of entering the crystal is taken as the axis of the cylinder. The length of the cylinder Δz_c is approximately 200 \AA . When the projectile approaches the end of the cylinder, a new cylinder is built as an extension of the previous one. The axis of the new cylinder is parallel to the new particle momentum. The procedure is repeated until the projectile reaches the end of the crystal. As a result, the cylinders form a ‘pipe’ filled with the crystal lattice and the particle moves in the middle of this ‘pipe’.

In the case of a bent crystal with channel shape defined by the function $y_B(z)$, the procedure of [41] is modified in the following way. If (x_p, y_p, z_p) are the coordinates of the projectile, and (x_c, y_c, z_c) is the endpoint of the cylinder axis:

$$\begin{aligned} z_c &= z_p + \Delta z_c \\ x_c &= x_p + \Delta z_c p_x / p_z \\ y_c &= y_p + \Delta z_c p_y / p_z. \end{aligned} \quad (1)$$

First, an undistorted lattice is built around the straight line segment connecting the points $(x_p, y_p - y_B(z_p), z_p)$ and $(x_c, y_c - y_B(z_c), z_c)$. Then each lattice node is shifted according to the bending profile:

$$(x_n, y_n, z_n) \rightarrow (x_n, y_n + y_B(z_n), z_n) \quad (2)$$

As a result, the trajectory becomes surrounded by a ‘pipe’ filled by the bent crystal lattice.

It is convenient to characterize the curvature of the bent crystal by the centrifugal parameter C [44]. Let $U(y)$ be the potential energy of the projectile in the field of straight crystal averaged over the coordinates x and z at

fixed y . Then the centrifugal parameter is defined as²

$$C = \frac{F_{c.f.}}{U'_{\max}}. \quad (3)$$

Here $F_{c.f.}$ is the centrifugal force acting on the projectile in the bent channel and U'_{\max} is the maximum derivative of the average potential energy with respect to y , i.e. the maximum force acting on the projectile in the average potential. The centrifugal force is related to the projectile energy E and to the bending radius R_C via $F_{c.f.} = E/R_C$. Therefore, expression (3) can be rewritten as

$$C = \frac{E}{R_C U'_{\max}}. \quad (4)$$

The shape of a channel with a constant bending radius is defined by the equation

$$y_B(z) = R_C - \sqrt{R_C^2 - z^2}. \quad (5)$$

In this case, the potential energy has to be averaged over the surface

$$y = y_B(z) + v \quad (6)$$

with fixed v .

With account for centrifugal effects, the potential energy of the particle has the form

$$U_{c.f.}(v) = U(v) - v F_{c.f.} \quad (7)$$

Because the crystal deformation is not very large, the modification of the electrostatic part of the potential energy can be neglected. Therefore, it is assumed that the function $U(v)$ in (7) does not depend on the crystal curvature. This is the reason, why U'_{\max} in (3) refers to the straight channel.

The average potential energy of the projectile in the field of bent crystallographic planes (110) with account for the centrifugal effects is shown in figure 1. It is seen from the figure and can be deduced from (3) and (7) that the value $C = 0$ corresponds to the straight crystal and $C = 1$ is the critical value at which the potential barriers between the crystal channels disappear.

The channel boundaries for a straight crystal are defined as the planes satisfying the equation $y = y_{\text{top}}^{(n)}$, where $y_{\text{top}}^{(n)}$ is the coordinate of the potential energy maximum between the n -th and $(n+1)$ -st channel. In the case of nonzero C , these planes become bent surfaces following the shape of the channel:

$$y = y_{\text{top}}^{(n)} + y_B(z). \quad (8)$$

In this case, the channel boundaries do not coincide with the maxima of the potential energy that are shifted due to the centrifugal effects (see figure 1).

² The continuous potential is not used in the simulation algorithm of the code ChaS. It is utilized only for the definition of the centrifugal parameter C .

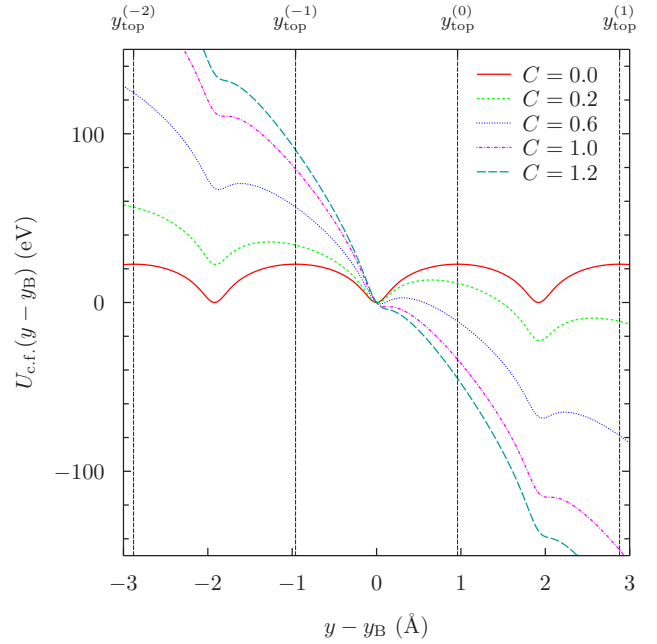


Fig. 1. The average potential energy of the projectile in the field of bent silicon crystal planes (110) with account for the centrifugal effects. The centrifugal parameter C is defined by equation (3).

3 Simulations

The simulations were performed for $E=855$ MeV electrons channeling along the plane (110) for a number of different values of C in the range from $C = 0$ to $C = 1.5$ (see table 1).

The case of an ideal zero-emittance beam entering the crystal strictly parallel to the coordinate axis z was simulated, i.e. the projectiles had zero transverse momentum at the entrance of the crystal. The initial transverse position of the projectile was chosen randomly, homogeneously distributed within a rectangular region. The y dimension of the rectangle was exactly equal to the channel width and the x dimension was of the same order of magnitude. Then the trajectory of the particle was simulated. The simulation of the trajectory was terminated if the particle went through the crystal: $z > L_c$, or if the deviation of the projectile from its initial direction became too large: $|\mathbf{p}_\perp|/p_z > 0.06 \gg \theta_L$. Here \mathbf{p}_\perp and p_z are, respectively, the transverse and the longitudinal momenta and θ_L is the critical (Lindhard's) angle, $\theta_L \approx 0.26 \cdot 10^{-3}$ rad for the channel (110) in silicon at $E = 855$ MeV.

Then the simulated trajectories were analyzed and the segments corresponding to channeling and dechanneling modes were determined. At the entrance point of the crystal, the projectile was assumed to be in the channeling mode. Regardless of the value of its transverse energy, the particle was considered to be channeling until it crossed the channel boundary (8).

The crystal dimensions along the beam direction L_c was chosen sufficiently large, so that practically all trajectories crossed the channel boundary at least ones, i.e.

Table 1. The parameters used in the simulations: the centrifugal parameter C , the crystal length L_c , and the number of simulated trajectories N_0 . The obtained values of the dechanneling length L_d and the asymptotic acceptance A_d (see section 4) are listed in the last two columns together with their statistical errors.

C	L_c (μm)	N_0	L_d (μm)	A_d
0.000	150	$2.0 \cdot 10^5$	8.401 ± 0.047	0.97 ± 0.01
0.025	130	$2.5 \cdot 10^4$	8.127 ± 0.099	0.92 ± 0.02
0.050	120	$2.5 \cdot 10^4$	7.417 ± 0.091	0.88 ± 0.02
0.075	110	$2.5 \cdot 10^4$	6.664 ± 0.010	0.83 ± 0.02
0.100	100	$2.5 \cdot 10^4$	5.995 ± 0.063	0.79 ± 0.01
0.150	90	$2.5 \cdot 10^4$	5.183 ± 0.066	0.68 ± 0.01
0.200	70	$2.5 \cdot 10^4$	4.298 ± 0.066	0.63 ± 0.02
0.250	60	$2.5 \cdot 10^4$	3.729 ± 0.056	0.57 ± 0.01
0.300	50	$2.5 \cdot 10^4$	3.304 ± 0.070	0.51 ± 0.02
0.400	35	$2.5 \cdot 10^4$	2.594 ± 0.052	0.45 ± 0.02
0.500	30	$5.0 \cdot 10^4$	1.988 ± 0.038	0.43 ± 0.02
0.600	25	$5.0 \cdot 10^4$	1.500 ± 0.018	0.43 ± 0.01
0.700	20	$5.0 \cdot 10^4$	1.176 ± 0.018	0.43 ± 0.01
0.800	15	$1.0 \cdot 10^5$	0.894 ± 0.011	0.44 ± 0.01
0.900	12	$1.0 \cdot 10^5$	0.640 ± 0.008	0.48 ± 0.01
0.950	12	$1.0 \cdot 10^5$	0.502 ± 0.007	0.57 ± 0.02
0.975	12	$1.0 \cdot 10^5$	0.440 ± 0.006	0.67 ± 0.02
1.000	10	$2.0 \cdot 10^5$	0.378 ± 0.005	0.84 ± 0.04
1.010	10	$2.0 \cdot 10^5$	0.349 ± 0.003	0.99 ± 0.03
1.025	8	$2.0 \cdot 10^5$	0.319 ± 0.003	1.14 ± 0.04
1.050	6	$2.0 \cdot 10^5$	0.264 ± 0.002	1.85 ± 0.05
1.100	5	$2.0 \cdot 10^5$	0.195 ± 0.002	4.13 ± 0.16
1.150	4	$2.0 \cdot 10^5$	0.149 ± 0.002	10.48 ± 0.61
1.200	3	$2.0 \cdot 10^5$	0.120 ± 0.001	26.40 ± 1.75
1.250	3	$2.0 \cdot 10^5$	–	–
1.300	3	$2.0 \cdot 10^5$	–	–
1.500	3	$2.0 \cdot 10^5$	–	–

all particles were already dechanneled at $z = L_c$. The rechanneling process (see [41] for a detailed discussion) takes place also in a bent channel. But it is irrelevant for the present analysis. The numerical values of L_c for each C as well as the numbers of simulated trajectories N_0 are listed in table 1.

4 The Dechanneling Length and the Asymptotic Acceptance of the Channel

To make a quantitative assessment of the particle dechanneling process, one needs a definition of the dechanneling length that would be suitable for the Monte Carlo approach. In this section, the definition of the dechanneling length proposed in [41] is reviewed and another useful quantity, the *asymptotic acceptance*, is introduced.

Let z_{d1} be the point of the first crossing of the channel boundary by the projectile trajectory. The quantity $N_{ch0}(z)$ is defined as the number of trajectories that satisfy the condition $z_{d1} > z$. In other words, this is the number of projectiles (among the total number N_0) that passed the distance from their entrance into the crystal to the point z in the channeling regime and dechannel at

some further point. The length $L(z)$ is the average distance from the point z to the first dechanneling point:

$$L(z) = \frac{\sum_{k=1}^{N_{ch0}(z)} (z_{d1}^{(k)} - z)}{N_{ch0}(z)}. \quad (9)$$

The sum in the numerator is taken over trajectories satisfying the condition $z_{d1} > z$.

Generally speaking, $L(z)$ depends not only on z , but also on the initial angular distribution of the particles. However, it has been demonstrated in [41] for strait channels that $L(z)$ reaches an asymptotic value at sufficiently large z . This value depends neither on z nor on the initial angular distribution. It will shown in the next section that $L(z)$ preserves this property in bent channels as well. The dechanneling length L_d is defined in the Monte Carlo procedure as the value of $L(z)$ given by (9) in the region where it ceases to depend on z . The number of channeling particles $N_{ch0}(z)$ decreases exponentially in this region

$$N_{ch0}(z) \asymp N_0 A_d \exp(-z/L_d). \quad (10)$$

Here N_0 is the total number of simulated trajectories.

Due to the exponential asymptote (10), the quantity

$$A(z) = \frac{N_{ch0}(z)}{N_0} \exp(z/L_d) \quad (11)$$

should also approach a constant value A_d at sufficiently large z . The quantity A_d will be called the *asymptotic acceptance* of the channel. Similar quantity can be defined also within the diffusion approach [45]. In contrast to the dechanneling length L_d , the asymptotic acceptance depends on the initial transverse momentum distribution of the particles in the beam.

The values of L_d and A_d calculated for the simulated trajectories are listed in table 1.

5 Analysis of the Results

The fraction $N_{ch0}(z)/N_0$ of the particles that reached the penetration depth z without crossing the channel boundary is shown in figure 2 as function of z for a few values of C . This fraction decreases rather fast and, as expected, it has an exponential asymptotic behavior. Surprisingly, the exponential tail is present also at $C = 1.025$. Qualitatively, the behavior of the ratio $N_{ch0}(z)/N_0$ for $C = 1.025$ is the same as for $C < 1$.

The quantity $L(z)$ defined by (9) for the same values of the centrifugal parameter as in figure 2 is plotted in figure 3. Indeed, $L(z)$ becomes constant (within the statistical errors) at large z corresponding the region of the exponential behavior of the curves in figure 2. This is valid for $C = 1.025$ as well as for $C < 1$. Only for $C > 1.2$ the asymptotic region with constant values of $L(z)$ could not be identified and the value of L_d could not be found.

The dependence of the ratio $L_d(C)/L_d(C=0)$ on the centrifugal parameter is shown in figure 4.

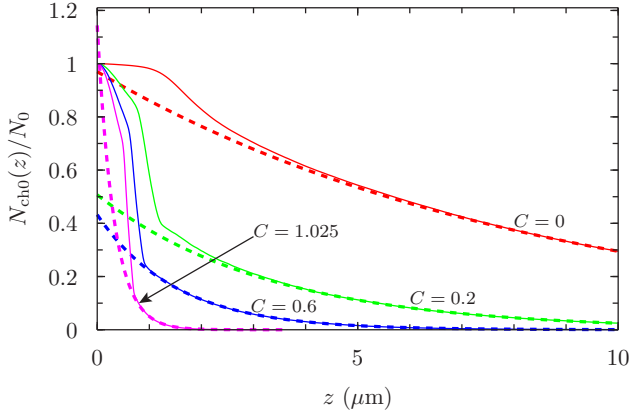


Fig. 2. The fraction $N_{\text{ch0}}(z)/N_0$ of the particles that did not cross the channel boundaries between their entrance into the crystal and the point z for different values of the centrifugal parameter C . The dashed lines show the corresponding exponential asymptotes $\propto \exp(-z/L_d)$.

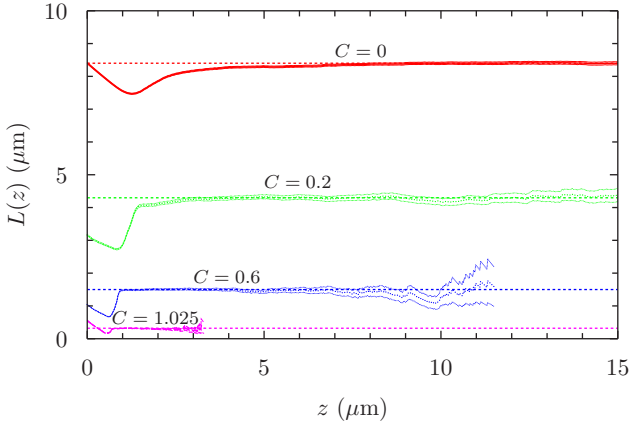


Fig. 3. The quantity $L(z)$ defined by (9) that becomes equal to the dechanneling length at large penetration depth z . The thin lines show the statistical errors. The straight dashed lines correspond to the asymptotic values.

It is seen from the figure that the ratio $L_d(C)/L_d(C=0)$ follows the law $(1-C)^{2.9}$ for $C \lesssim 0.3$. At $C \gtrsim 0.3$, it decreases less steeply and remains nonzero even at $C > 1$.

The quantity $A(z)$ defined by (11) is plotted in figure 5. This quantity indeed approaches a constant value in the same region of z where the quantity $L(z)$ does. By definition, this value is the asymptotic acceptance A_d of the channel for an ideally parallel beam. Qualitatively, the behavior of the curve in the asymptotic region is the same for $C = 1.025$ as for $C < 1$.

The dependence of the ratio $A_d(C)/A_d(C=0)$ on the centrifugal parameter is shown in figure 6. It is seen from the figure that the behavior of the ratio is changed at $C = 0.3$: it falls as $(1-C)^2$ at $0 \lesssim C \lesssim 0.3$ then it becomes nearly constant at $0.3 \lesssim C \lesssim 0.8$. Finally, the ratio starts to grow at $C \gtrsim 0.8$ and becomes larger than unity at $C > 1$. The last four points lie outside the the upper bound of the vertical axis and, therefore, they are not shown in the figure. Because the value of L_d is necessary for calculation

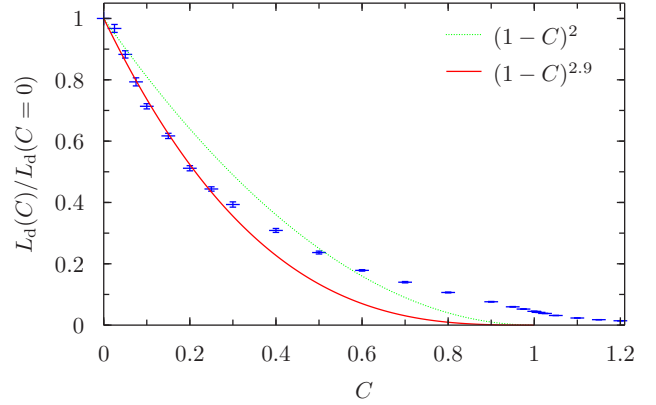


Fig. 4. The ratio $L_d(C)/L_d(C=0)$ of the dechanneling length in bent channels to the one in the straight channels as function of the centrifugal parameter C . At $C \lesssim 0.3$ the ratio can be parametrized by the function $(1-C)^{2.9}$ (shown by the solid line). For comparison, the behavior $(1-C)^2$ obtained in the diffusion theory in the parabolic potential approximation [45] is shown by the dashed line.

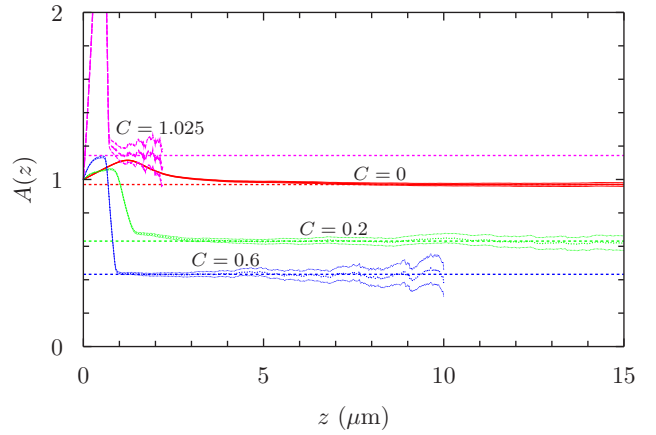


Fig. 5. The quantity $A(z)$ defined by (11) that becomes equal to the asymptotic acceptance of the channel at large penetration depth z . The thin lines show the statistical errors. The straight dashed lines correspond to the asymptotic values A_d .

of $A(z)$ (see (11)), the asymptotic acceptance A_d could not be found for $C > 1.2$.

Examples of trajectories with large channeling segments are shown in figure 7. In the case of a small centrifugal parameter, $C = 0.2$, the trajectory oscillates around the minimum of the continuous potential. The amplitude and the phase of the oscillations are fluctuating due to the incoherent scattering. Nonetheless, the oscillation pattern is clearly seen.

No oscillations are observed at a large centrifugal parameter, $C = 1.025$. Instead, the particle is being randomly scattered. The channeling segment of a trajectory can be much larger than average, if random scatterings happen to keep the particle in the region of the gentlest slope of the centrifugally modified continuous potential $U_{\text{c.f.}}(v)$ defined by (7) (cf. figure 1). Exactly this case is shown in the lower panel of figure 7.

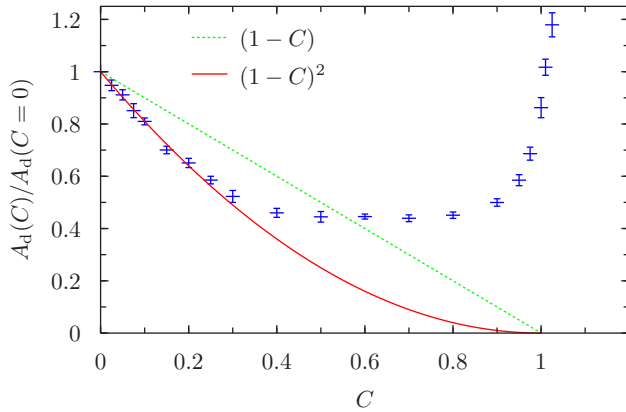


Fig. 6. The ratio $A_d(C)/A_d(C=0)$ of the asymptotic acceptance of bent channels to the one in the straight channel as function of the centrifugal parameter C . At $0 \lesssim C \lesssim 0.3$ the ratio can be parametrized by the function $(1-C)^2$ (shown by the solid line). For comparison, the behavior $(1-C)$ obtained in the diffusion theory in the parabolic potential approximation [45] is shown by the dashed line.

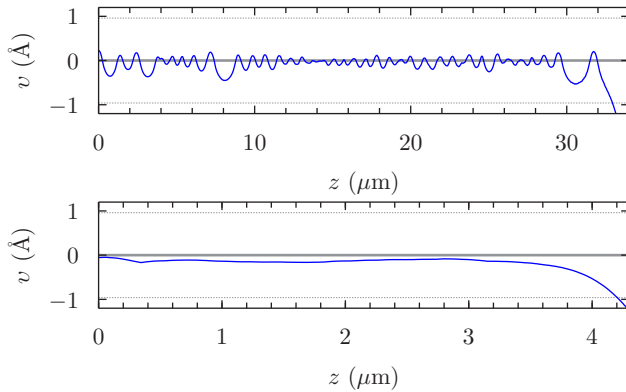


Fig. 7. Examples of simulated trajectories for $C = 0.2$ (upper panel) and $C = 1.025$ (lower panel). In each case, the trajectory having the largest channeling segment was chosen among thousands of simulated ones. The vertical coordinate is $v = y - y_B(z)$, cf. (6). The thick gray lines stand for the crystal planes. The thin dashed lines are the channel boundaries.

The cases $C < 1$ and $C > 1$ seem to look completely different if one thinks about them in terms of the continuous potential approximation. Indeed, the channeling of the particle would continue indefinitely long at $C < 1$ if one considers the continuous potential and neglects the incoherent collisions. In contrast, all the particles would dechannel quickly if one uses the same approximation at $C > 1$. The effect of the incoherent collisions seems to be opposite in these two cases. They result into dechanneling of the projectiles at $C < 1$. On the other hand, the incoherent scattering prevents a substantial fraction of projectiles from immediate dechanneling at $C > 1$. These projectiles form the exponential tail that is seen in figure 2 for $C = 1.025$.

Surprisingly, there is no abrupt transition between these two seemingly different pictures. The behavior of the curves in figures 2, 3 and 5 is qualitatively the same

for $C < 1$ and $C > 1$. No singularity is seen at $C = 1$ in figures 4 and 6. Separation of the projectile scattering into coherent and incoherent contributions that led us to two different pictures seems to be misleading in this situation.

One might wonder whether the term ‘channeling’ is eligible in the case $C > 1$. Indeed, there is no potential barriers between the channels. Therefore, the notion of channel becomes purely geometrical rather than physical. Still, there is a measurable physical effect that legitimize using the word channeling in the ‘supercritical’ regime $C > 1$.

The transverse momentum of projectile p_y averaged over all simulated trajectories, regardless whether they are channeling or dechanneled, is plotted in figure p_y versus the longitudinal coordinate z . It is seen that a bent crystal preserves its guiding properties even at $C > 1$. Moreover, a small steering effect is present even at $C = 1.5$, although the values of L_d and A_d could not be determined in this case.

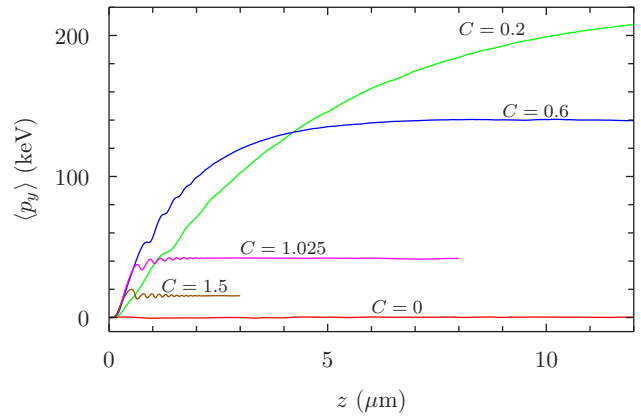


Fig. 8. The transverse momentum p_y of the projectile averaged over all simulated trajectories as function of the penetration depth z for different values of the centrifugal parameter C .

At the same time, one has to conclude that the ‘supercritical channeling’ is not the most interesting case from the practical point of view. Electron beams can be steered more effectively using bent crystal channels with moderate values of the centrifugal parameter $C = 0.2-0.3$.

6 Conclusion and Discussion

A Monte-Carlo study of electron channeling in the (110) channel of a bent silicon crystal is presented. The calculations were done for the beam energy of 855 MeV for a number of values of the centrifugal parameter.

According to the simulation results, the fraction of channeling electrons decreases rapidly with the penetration depth z and quickly approaches an exponential asymptote. Similar behavior was previously seen for straight channels [41]. This result is consistent with the one obtained in the kinetic theory of channeling in the case of positively charged projectiles [45].

A definition of the asymptotic acceptance of the channel A_d that is suitable for application within the Monte Carlo approach is formulated. The dependence of A_d on the centrifugal parameter is studied.

The dechanneling length for a set of values of the centrifugal parameter is calculated. It decreases as $\sim (1 - C)^{2.9}$ at $0 < C \lesssim 0.3$. At $C > 0.3$ it decreases less steeply and remains nonzero even at $C > 1$.

The behavior of the asymptotic acceptance $A_d(C)$ changes from decreasing, $A_d(C) \propto (1 - C)^2$, at $C \lesssim 0.3$ to nearly flat behavior at $0.3 \lesssim C \lesssim 0.8$. Then it starts to increase at $C \gtrsim 0.8$.

It is shown that a bent crystal preserves its steering properties even at 'supercritical' values of the centrifugal parameters $C > 1$. However, the guiding effect is stronger, if a bent crystal with a moderate value of C is used.

It can be concluded from the above properties of electron channeling in the bent crystal that the period of the crystalline undulator should not exceed several microns if one would like to observe the undulator effect using the electron beam with the energy in the range of hundreds of megaelectronvolt. The centrifugal parameter should not be larger than $C = 0.2$ – 0.3 , otherwise almost all projectiles will dechannel before the completion of the first undulator period and, therefore, will not contribute to the undulator radiation.³

The obtained result may be also useful for choosing the optimum bending of the crystals used for deflection and collimation of electron beams.

Acknowledgement

At its initial stage, the work was done in the Frankfurt Institute for Advanced Studies (FIAS) and was supported by the Deutsche Forschungsgemeinschaft (DFG). The numerical simulations were done at the Center for Scientific Computing of the J.W. Goethe University, Frankfurt.

References

1. J. Lindhard, Kong. Danske Vid. Selsk. Mat.-Fys. Medd. **34**(14) (1965) 1–64.
2. E.N. Tsyanov, TM-682, TM-684, Fermilab, Batavia (1976).
3. A.F. Elishev *et al.*, Phys. Lett. B **88** (1979) 387–391.
4. V.A. Andreev *et al.*, Pis'ma Zh. Eksp. Teor. Fiz. **36** (1982) 340–343 (JETP Lett. **36** (1982) 415–419).
5. A.M. Taratin and S.A. Vorobiev, Phys. Lett. A, **119** (1987) 425–428.
6. A.G. Afonin *et al.*, Nucl. Instrum. Meth. B **234** (2005) 14–22.
7. G. Arduini *et al.*, Phys. Lett. B **422** (1998) 325–333.
8. R.A. Carrigan *et al.*, Phys. Rev. ST Accel. Beams **5** (2002) 043501.
9. R.P. Fliller *et al.*, Phys. Rev. ST Accel. Beams **9** (2006) 013501.
10. S. Stokov *et al.*, J. Phys. Soc. Jap. **76** (2007) 064007.
11. W. Scandale *et al.*, Phys. Rev. ST Accel. Beams **11** (2008) 063501.
12. W. Scandale, G. Arduini, R. Assmann, C. Bracco, F. Cerutti, J. Christiansen, S. Gilardoni and E. Laface *et al.*, Phys. Lett. B **703** (2011) 547.
13. W. Scandale, Mod. Phys. Lett. A **27** (2012) 1230007.
14. E. Uggerhøj and U.I. Uggerhøj, Nucl. Instrum. Meth. B **234** (2005) 31.
15. S. Bellucci *et al.*, Nucl. Instrum. Meth. B **252** (2006) 3–6.
16. S. Stokov *et al.*, Nucl. Instrum. Meth. B **252** (2006) 16.
17. W. Scandale *et al.*, Phys. Rev. A **79** (2009) 012903.
18. V. V. Kaplin, S. V. Plotnikov and S. A. Vorobiev, Zh. Tekh. Fiz. **50** (1980) 1079–1081, (Sov. Phys. Tech. Phys. **25** (1980) 650–651).
19. V. G. Baryshevsky, I. Ya. Dubovskaya and A. O. Grubich, Phys. Lett. A, **77** (1980) 61–64.
20. A. Kostyuk, Phys. Rev. Lett. **110** (2013) 115503.
21. A. V. Korol, A. V. Solovov and W. Greiner, Int. J. Mod. Phys. E **8**, 49 (1999).
22. M. Tabrizi, A. V. Korol, A. V. Solov'yov and W. Greiner, Phys. Rev. Lett. **98** (2007) 164801.
23. M. Tabrizi, A. V. Korol, A. V. Solov'yov and W. Greiner, J. Phys. G **34** (2007) 1581.
24. X. Artru, Nucl. Instrum. Meth. B **48** (1990) 278.
25. V. Biryukov, Phys. Rev. E **51** (1995) 3522.
26. V.O. Bogdanov *et al.*, J. Phys.: Conf. Ser. **236** (2010) 012029.
27. V. Guidi, A. Mazzolari and V. Tikhomirov, J. Appl. Phys. **107** (2010) 114908.
28. A. V. Korol, A. V. Solovov and W. Greiner, J. Phys. G **27** (2001) 95.
29. K. Saitoh, J. Phys. Soc. Japan, **54** (1985) 152.
30. A.M. Taratin, E.N. Tsyanov and S.A. Vorobiev, Phys. Lett. A **72** (1979) 145.
31. M. T. Robinson and O. S. Oen, Appl. Phys. Lett. **2** (1963) 30; Phys. Rev. **132** (1963) 2385.
32. V.V. Kudrin, Yu. A. Timoshenkov and S.A. Vorobiev, Phys. Stat. Sol. B **58** (1973) 43.
33. S. K. Andersen *et al.*, Nucl. Phys. B **167** (1980) 1.
34. J. F. Bak *et al.*, Nucl. Phys. B **242** (1984) 1.
35. P.J.M. Smulders and D.O. Boerma, Nucl. Instrum. Meth. B **29** (1987) 471.
36. M.B.H. Breese, Nucl. Instrum. Meth. B **132** (1997) 540–547.
37. U. Mikkelsen and E. Uggerhøj, Nucl. Instrum. Meth. B **160** (2000) 435–439.
38. A. Kostyuk, arXiv:1301.4491 [physics.acc-ph].
39. H. Backe, P. Kunz, W. Lauth and A. Rueda, Nucl. Instrum. Meth. B **266** (2008) 3835–3851.
40. H. Backe, Nuovo Cimento C, **34**(4) (2011) 157–165.
41. A. Kostyuk, A. Korol, A. Solov'yov and W. Greiner, J. Phys. B **44** (2011) 075208.
42. N.F.M. Henry and K. Lonsdale (eds), International tables for x-ray crystallography, (The Kynoch Press, Birmingham, 1965).
43. G. Molière, Z. Naturforschung A **2** (1947) 133–145.

³ The results of the present study are relevant if the undulator period is longer than the period of the channeling oscillations. For a very short bending period (in the range of hundreds of nanometers), the channeling is possible even for very large values of the centrifugal factor C , provided that the bending amplitude is smaller than the channel width [20].

- 44. A. V. Korol, A. V. Solov'yov and W. Greiner, *Int. J. Mod. Phys. E* **13** (2004) 867.
- 45. V. M. Biryukov, Yu. A. Chesnokov, V. I. Kotov. *Crystal Channelling and its Application at High-Energy Accelerators* (Springer, Berlin, Heidelberg, New York, 1996)